J. Fluid Mech. (1993), *vol.* 254, *pp.* 363–374

Observations on transition in plane bubble plumes

By M. ALAM AND V. H. ARAKERI
Department of Mechanical Engineering, Indian Institute of Science, Bangalore 560 012, India

(Received 31 January 1992 and in revised form 24 March 1993)

Flow visualization studies of plane laminar bubble plumes have been conducted to yield quantitative data on transition height, wavelength and wave velocity of the most unstable disturbance leading to transition. These are believed to be the first results of this kind. Most earlier studies are restricted to turbulent bubble plumes. In the present study, the bubble plumes were generated by electrolysis of water and hence very fine control over bubble size distribution and gas flow rate was possible to enable studies with laminar bubble plumes. Present observations show that (*a*) the dominant mode of instability in plane bubble plumes is the sinuous mode, (*b*) transition height and wavelength are related linearly with the proportionality constant being about 4, (*c*) wave velocity is about 40% of the mean plume velocity, and (*d*) normalized transition height data correlate very well with a source Grashof number. Some agreement and some differences in transition characteristics of bubble plumes have been observed compared to those for similar single-phase flows.

1. Introduction

When gas bubbles are released in the interior of an otherwise stagnant liquid, they rise owing to buoyancy entraining the surrounding liquid to form what can be termed as a 'bubble plume'. Large-scale bubble plumes have found some applications like bubble breakwaters as originally suggested by Taylor (1955); they have also been used to prevent parts of the surface of a river or lake from freezing over (Baines 1961) and in containment of oil slicks (Jones 1972). In addition, a desire to understand the hydrodynamics of undersea blowouts has stimulated some recent studies on bubble plumes. A comprehensive review of the state of the art in understanding and predicting the mean flow characteristics of turbulent large-scale round bubble plumes has been provided by Milgram (1983). Typically, large-scale bubble plumes of the type studied by Milgram involve heights which are in the range of few metres and gas flow rates which are fractions of a cubic metre per second.

At the other end of the spectrum are small-scale bubble plumes where heights are in the range of a few centimeters and gas flow rates are a few centimeters cubed per second or smaller. These find application in chemical and metallurgical processing industries (Leitch & Baines 1989). If the bubble sizes involved are a few millimeters, even the weak bubble plumes of the type investigated by Leitch & Baines turn out to be turbulent. In fact, there are hardly any studies involving laminar and transitional bubble plumes. It is felt that studies in this direction could provide a data base for comparison with modelling of two-phase flow equations where there are still some unsettled questions regarding the handling of the dispersed phase (van Wijngaarden 1972; Ishii 1975). These questions can perhaps be investigated in a more meaningful manner by studying laminar or transitional bubble plumes than their turbulent counterparts where there are additional complexities. These considerations have

formed the primary motivation for the present study where we have observed in some detail the transition process in two-dimensional or plane bubble plumes. A new technique had to be evolved to generate laminar bubble plumes in a low-viscosity fluid like water, since standard methods like release of gas bubbles through a set of needles or a porous plug result in turbulent bubble plumes as indicated in Leitch & Baines (1989).

The new technique is described in §2, which is followed by presentation of results and their discussion in §3. In §4 a normalized representation of transition height data is attempted and, finally, a summary of the important findings is contained in §5.

2. Experimental methods

Bubble plumes in the present study were generated by electrolysis of water from a specially fabricated electrode configuration. The cathode was a strip of conducting surface of different base width D_0 and length L which was prepared on a copper-clad laminate sheet (generally used for printed circuit boards) by etching out the unwanted portion. Fine control of the dimensions of width and length was possible by the use of printed circuit board technology. A schematic of an array of seven cathode strips etched on a laminate is shown in figure 1 (it should be noted that this configuration was chosen since both transition and interaction studies were contemplated, Alam 1991). Such a laminate was flush mounted on a perspex holder and placed inside a square based glass tank of sides 40 cm each and a height of 75 cm. The anode was a separate unetched laminate and was placed below the perspex holder with its conducting surface facing downwards as shown schematically in figure 1. Thus, with the application of a d.c. voltage between the electrodes, the cathode acted as a 'bubble generator' for hydrogen bubbles. Since the anode was placed facing downwards, the oxygen bubbles liberated at the anode could not escape to interact with the buoyantly rising hydrogen bubble plume.

For studying the structure and development of the bubble plume, it was illuminated by a narrow (thickness 2–3 mm) bright sheet of light and both still and motion pictures (framing rate of 1.5 frames per s) were recorded with the help of a motor-driven 35 mm camera at an oblique angle of about 110°–115° (see figure 1). The plume appeared brightest at this angle. Most of the photographs were obtained with illumination angle as shown schematically in figure 1. However, a few photographs were also recorded by lighting the plume along the lengthwise or spanwise direction. This was done to verify the two-dimensionality of the plume structure.

In addition to plume flow visualization using light-sheet technique, measurements were made of the plume centreline velocity using a DISA one-component laser-Doppler anemometer (LDA). The LDA was used in the forward-scatter mode and the general arrangement is depicted in figure 1. Certain precautions had to be taken to obtain reasonably accurate mean plume velocities since it was observed that the plume centreline wandered in a seemingly random manner. Basically, instantaneous velocity readings were noted down when the plume centreline coincided with the probe volume and these were subsequently averaged. The difficulties experienced here appear to be a common feature of bubble plumes as discussed by Milgram (1983). The reasons for plume wandering in the present case may, however, be different from the ones for axisymmetric turbulent bubble plumes.

One of the primary variables in the present study was the gas flow rate per unit length, Q_g which ranged from 0.004 $mm^3\ s^{-1}\ mm^{-1}$ to 0.09 $mm^3\ s^{-1}\ mm^{-1}$ for one of the cathode configurations. Gas flow rate was computed using Faraday's law and the

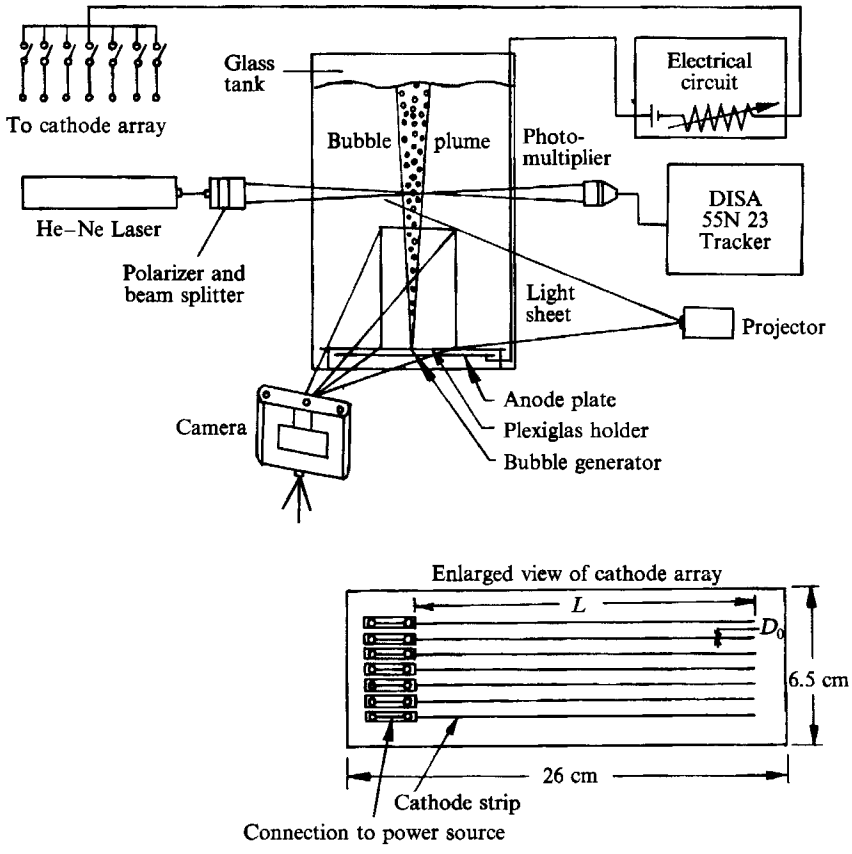

FIGURE 1. Schematic sketch of the experimental set-up and details of the cathode array.

measured current in the circuit. The other variable was the width of the cathode electrode, D_0, for which three values were chosen, namely 1.7, 1.0 and 0.4 mm. For the 1.7 mm electrode, three different lengths, $L(= 17,\ 8.5$ and 4.25 cm) were used. However, preliminary investigations (see Alam 1991 for more details) showed that if length L equalled or exceeded the value of 8.5 cm two-dimensionality was achieved. Here, two-dimensionality implies that quantities like transition height did not change with L if its value was such that $L/D_0 > 50$. In view of this, results from a common length L of 8.5 cm for the 1.7, 1.0 and 0.4 mm electrodes are presented here.

For a given electrode width, it was found that if the gas flow rate exceeded a certain value there was a dramatic change in the plume structure. Close observation with stroboscopic illumination indicated that this was due to the coalescence of bubbles at the source. At gas flow rates lower than this upper limit, coalescence was not predominant and this was verified by photographing bubble sizes at various heights. One of the significant aspects of the present technique of bubble plume generation was the small size of the bubbles and the narrow range of bubble size distribution. Typically, as reported in Alam (1991), the mean bubble diameter was 120 μm for a gas flow rate Q_g of 0.0144 $\text{mm}^3\ \text{s}^{-1}\ \text{mm}^{-1}$ and 130 μm at Q_g of 0.072 $\text{mm}^3\ \text{s}^{-1}\ \text{mm}^{-1}$. In both cases, the standard deviation was about 20 μm. These bubble sizes correspond to low Eötvös and Reynolds number (1–3) and from Clift, Grace & Weber (1978, figure 2.5) they are expected to remain spherical and move in a rectilinear path. Therefore, very little or no disturbance was introduced in the plume due to unsteadiness of an

individual bubble path or its wake. It should be noted that in the present experiments small bubbles are naturally produced and this ensures homogeneity of the mixture. In contrast, McDougall (1978) had to use additives to reduce the size of the bubbles in his studies on bubble plumes. The present plumes correspond to very low-void-fraction bubble plumes but still appear homogeneous for the reason just indicated. Following Arakeri & Nair (1990), using drift flux theory the void fraction near the source, ϵ_0 can be estimated as $\epsilon_0 = Q_g/U_\infty D_0$; here, Q_g is the gas flow rate per unit source length, U_∞ is the terminal velocity of a single bubble and D_0 is the width of the source. Typical values of ϵ_0 range from 3×10^{-4} to 8×10^{-3}; in addition, an estimate for the interbubble distance is of the order of 3–4 bubble diameters. This is unlikely to lead to coalescence in the absence of some forcing mechanism like turbulent fluctuations. In fact, ready coalescence was observed if the plume was excited with high-frequency sound.

All the present experiments were conducted with filtered tap water at a temperature of 25 °C. The water height H_0 in the tank was varied from 20 to 50 cm; however, most of the results presented here are for H_0 of 50 cm since the variation of water height had only marginal influence on the findings (Alam 1991).

3. Results and discussion

3.1. *Flow visualization*

One of the major purposes of the present study was to document the natural transition process from laminar to turbulent flow in a plane bubble plume. A series of photographs showing some of the typical characteristics of the transition process are shown in figures 2–4. Additional photographs may be found in Alam (1991).

In figure 2 the plume structure at two different gas flow rates is shown. It is clear that initially the bubble core remains compact and appears straight; however, at a certain distance from the source sinusoidal instabilities develop which amplify in the downstream direction to result in the sudden loss of the compactness of the bubbly core. At higher gas flow rates the compactness is lost at a shorter height accompanied by formation of discrete alternate vortices; however, discrete vortices do not form at smaller gas flow rates. In either case, the loss of compactness with or without formation of discrete vortices was taken to signify transition to turbulence. In fact, with low water height and small gas flow rates, the bubble plume remained laminar for the entire height. Figure 3(*a*) clearly shows this and other photographs highlight the features just described. In figure 3(*e*) a clear alternating vortex structure is observed. It should be noted that, since the photographs were taken at an oblique angle that is not 90°, the bubble core thickness of the plume is not correctly depicted in the photographs of figures 2 and 3. However, quantities like transition height and wavelength can be measured accurately from this oblique view. This fact was verified by taking additional photographs with a 90° viewing angle.

Figure 4 shows the spanwise view of the bubble plume at two different gas flow rates. What is actually depicted in the photographs is the core region of the plume occupied by bubbles. There is of course additional entrained liquid flow which is not visualized; special techniques other than dye injection may be required to observe this since the velocities involved are extremely low. The dark line in the photographs is a reference height mark and the arrows indicate the location of transition as obtained from photographing the plume in the manner desribed above. It is clear that the initial region including the laminar and beginning stages of instability is two-dimensional. However, later stages of transition do show three-dimensionality. In figure 4(*a*), the bulges are out of phase along the spanwise direction; it is interesting to note that there

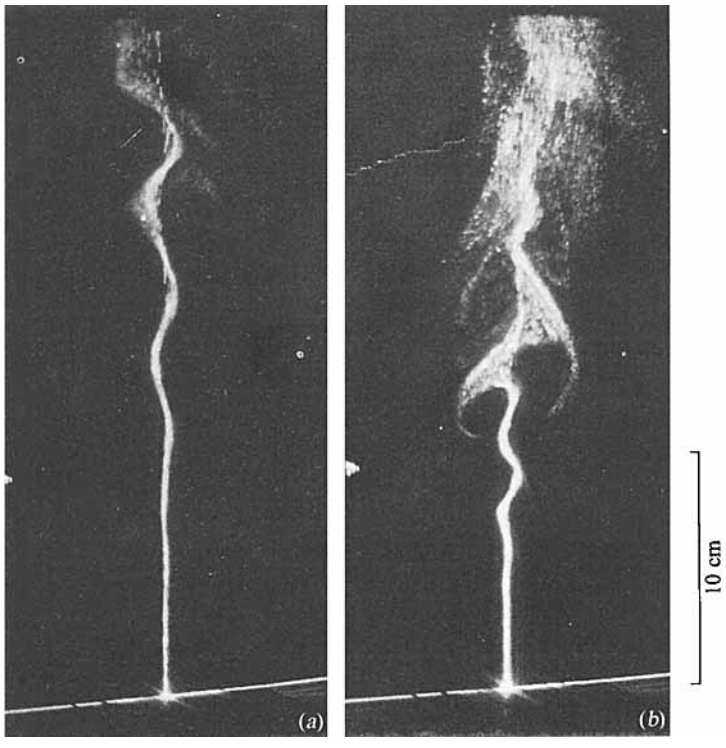

FIGURE 2. Sinuous instability of plane bubble plumes ($L = 8.5$ cm, $D_0 = 1.7$ mm, $H_0 = 50$ cm). The photographs show the cross-sectional view of the bubble core region: (*a*) $Q_g(\times 10^3) = 4.3$ mm^3 s^{-1} mm^{-1}; (*b*) 18.0 mm^3 s^{-1} mm^{-1}.

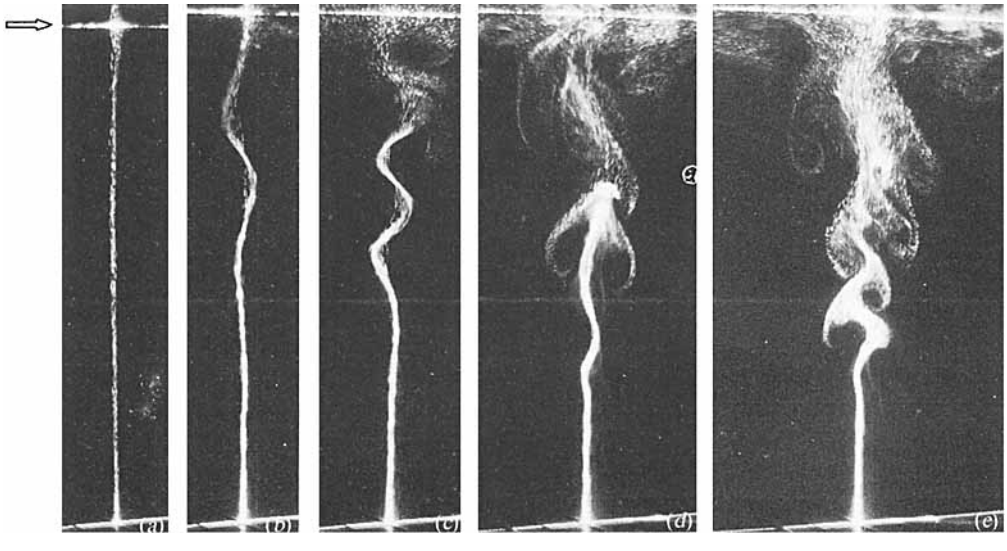

FIGURE 3. Effect of gas flow rate on transition characteristics of plane bubble plumes ($L = 8.5$ cm, $D_0 = 1.7$ mm, $H_0 = 20$ cm): (*a*) $Q_g(\times 10^3) = 3.7$ mm^3 s^{-1} mm^{-1}; (*b*) 7.4 mm^3 s^{-1} mm^{-1}; (*c*) 11.1 mm^3 s^{-1} mm^{-1}; (*d*) 18.5 mm^3 s^{-1} mm^{-1}; (*e*) 37.0 mm^3 s^{-1} mm^{-1}. The arrow in (*a*) indicates the location of the free surface.

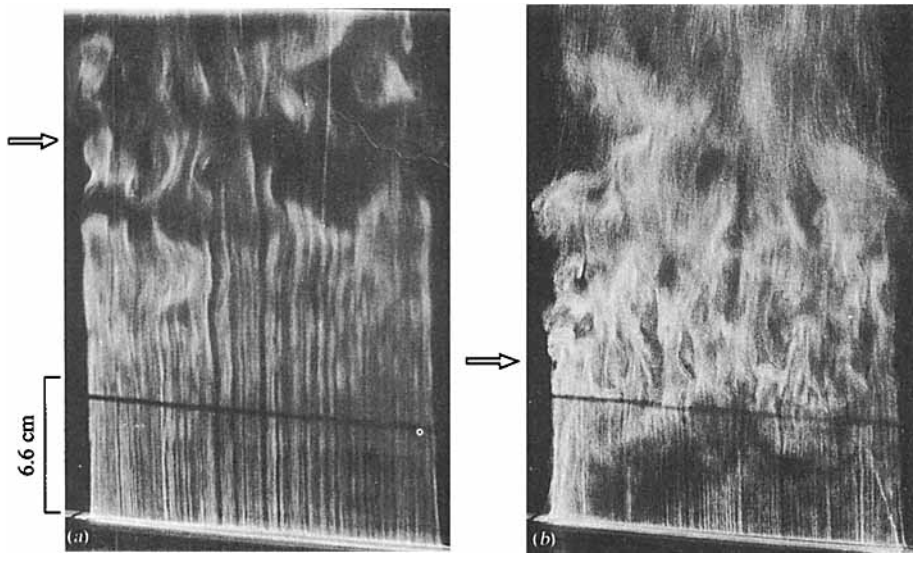

FIGURE 4. Spanwise view of bubble plumes ($L = 17$ cm, $D_0 = 1.7$ cm, $H_0 = 50$ cm): (*a*) $Q_g(\times 10^3) = 9.0$ mm^3 s^{-1} mm^{-1}; (*b*) 38.5 mm^3 s^{-1} mm^{-1}. The arrows indicate the location of transition.

are none of the noticeable end effects which are prominent in thermal plumes (Schorr & Gebhart 1970). The photographs in figure 4 show a prominent streak-like structure in the laminar portion which remains unexplained. An instability in the release mechanism may be responsible for this.

The primary instability associated with present bubble plumes seems to closely resemble that in thermal plumes. Sinuous or meandering motion has been clearly documented for both plane and axisymmetric thermal plumes (Wakitani & Yosinobu 1988; Bill & Gebhart 1975; Kimura & Bejan 1983). This type of motion is more distinct in high Prandtl number fluids like spindle oil as compared to air. In this connection it should be noted that the present bubble plumes correspond to an equivalent high Prandtl number limit since there is no ready mechanism for lateral diffusion of bubbles in the laminar region, thus resulting in very little spread of the bubble core.

3.2. *Transition height and wavelength*

From photographs of the type shown in figures 2 and 3, it was possible to measure the transition height X (based on the criterion mentioned in §3.1) and the wavelength λ of the disturbance leading to transition. This is also the wavelength which has received the maximum amplification. It is well known that transition is sensitive to extraneous parameters and hence we carried out extensive checks on the repeatability of our results. These are detailed in Alam (1991) but significant aspects are mentioned below. We found that the data for the transition height could be reproduced to within about 5–10% for a given gas flow rate. This included day-to-day variations and measurement of transition height at different spanwise locations. The variation in the measured value of the unstable wavelength was larger, being of the order of 15–25% in particular at low gas flow rates. Both X and λ were not influenced by the variation in the free-surface height of the water in the tank. Some transition height measurements were made as the plume developed, in the sense that the plume front had not reached the free surface at the time of measurement (this is similar to a 'starting plume'). It was found that the

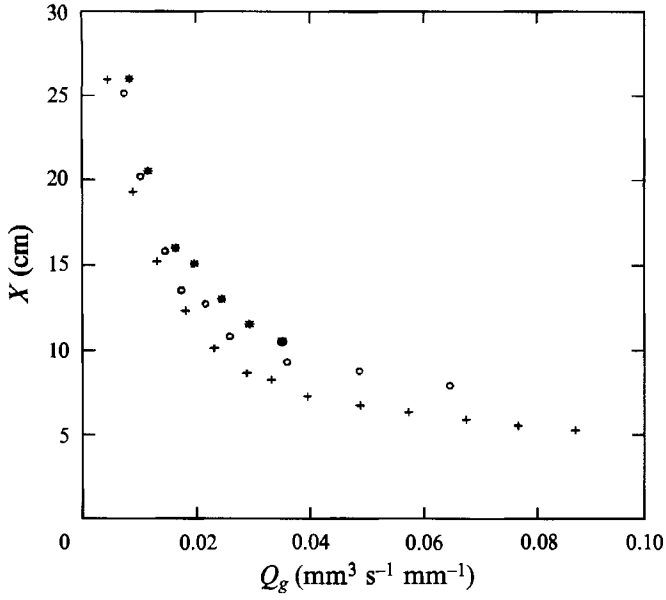

FIGURE 5. Effect of gas flow rate on transition height: *, $D_0 = 0.4$ mm; ○, 1.0 mm; +, 1.7 mm.

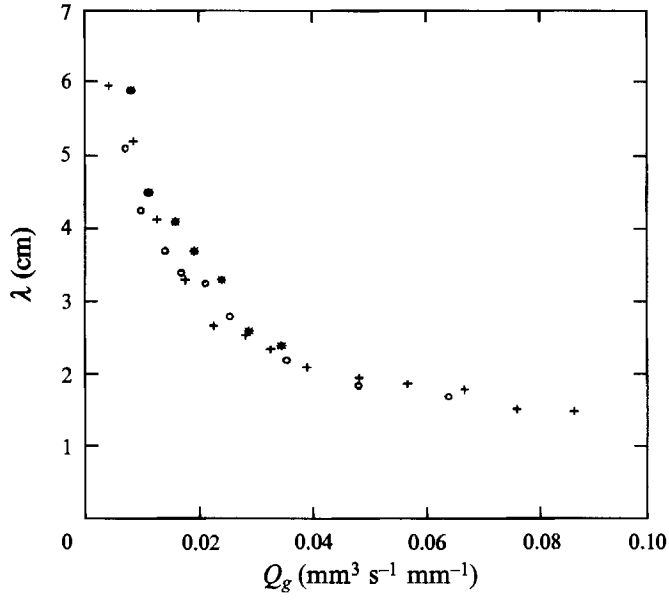

FIGURE 6. Effect of gas flow rate on the magnitude of the wavelength: symbols as figure 5.

transition height measurements under these conditions agreed with those of the steady-state bubble plume within the error band noted above. This last observation clearly indicates that the recirculating flow in the tank was too weak to significantly influence the transition process observed.

The variation of X and λ with different Q_g for various electrode geometries used are shown in figures 5 and 6 respectively. It should be noted from these figures that X varies distinctly when D_0 is varied at a nearly fixed value of Q_g, whereas this is not apparent

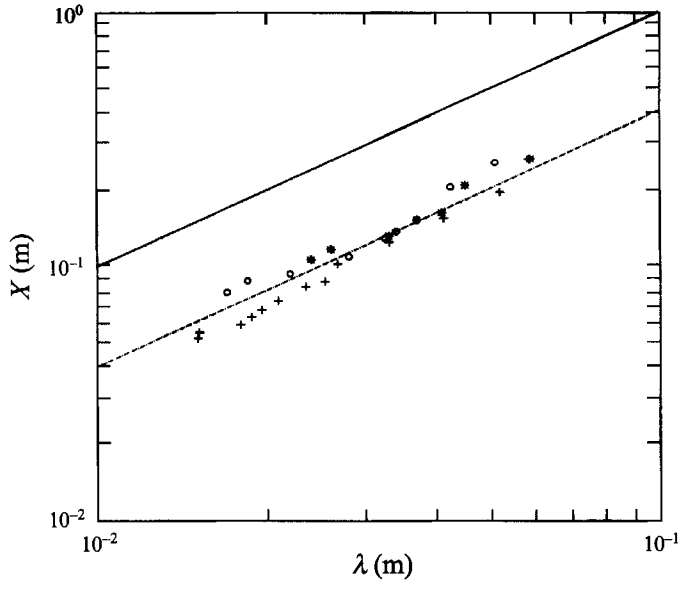

FIGURE 7. Relationship between transition height X and wavelength λ: symbols as figure 5; ---, $X = 4\lambda$; ——, $X = 10\lambda$.

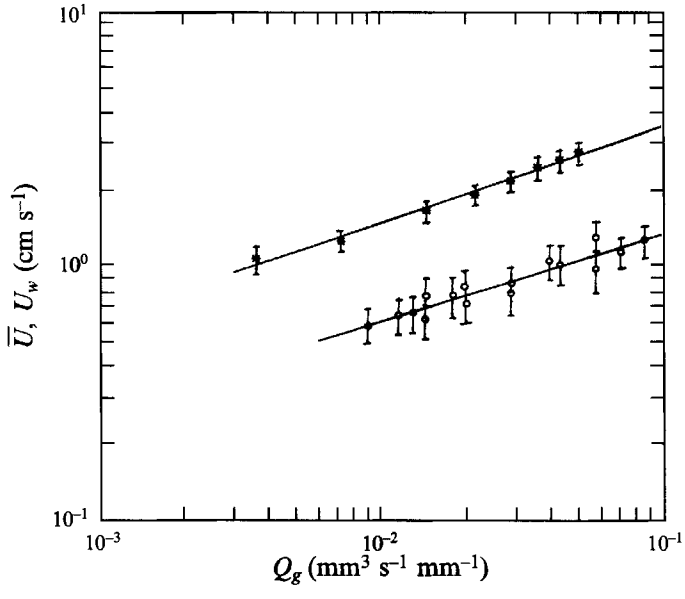

FIGURE 8. Variation of plume centreline velocity $\bar{U}$(*) and wave velocity U_w(○) on gas flow rate ($D_0 = 1.7$ mm).

for λ. This may be due to the larger scatter in the measured values of λ as compared to X, as pointed out earlier. The variation of both X and λ with Q_g is similar and it was found that they are linearly related with the proportionality constant being of the order of 4. This is shown in figure 7. For axisymmetric thermal plumes, Kimura & Bejan (1983) have found the proportionality constant to be of the order 10. In addition, recently Gore, Crowe & Bejan (1990) have shown that the proportionality $X \sim 10\lambda$ is

satisfied in a wide class of flows and for comparison this relationship is also shown in figure 7. The differing constant of proportionality is one of the significant departures of the present two-phase flow observations as compared to findings in similar single-phase flows.

3.3. *Wave and mean plume velocity*

The measured wave and mean plume centreline velocities are presented in figure 8. The wave speed U_w was obtained from motion picture studies of the plume and the mean centreline velocity $\bar{U}$ in the plume at a height of 5 cm was obtained using LDA. Note that at this measuring station ($H = 5$ cm), the plume remains laminar for the range of gas flow rates studied. The estimated terminal velocity U_∞ from bubble size measurements is of the order of 1 cm/s and hence significantly smaller than $\bar{U}$. It is seen that the dependence of U_w and $\bar{U}$ on Q_g are similar, suggesting a linear relationship between the two. From the results in figure 8, the constant of proportionality in the relationship $U_w = k\bar{U}$ is found to be of order 0.4. For single-phase flows in jets and mixing layers, k has been found to be of the order of 0.5 (Michalke 1965; Brown & Roshko 1974). From the knowledge of U_w and λ we can estimate the frequency f of the unstable waves as $f = U_w/\lambda$; the range of f is found to be 0.07 to 0.85 Hz.

4. Non-dimensional representation of transition height data

In the present case a functional relationship between X, the transition height, and the local plume variables can be expressed as

$$F[X, (\rho_l - \rho_g), (\rho_l - \rho_p), g, D_0, \mu, U_s] = 0.$$

Here, ρ_l is the liquid density, ρ_g the gas density, ρ_p the plume density, g the acceleration due to gravity, D_0 the width of the source, μ the coefficient of dynamic viscosity of the liquid and U_s the bubble slip velocity. We have not included some additional parameters that Milgram (1983) considered and the justification for this follows. In turbulent bubble plumes of the type analysed by Milgram, the stable bubble size is determined by the surface tension effects and hence the coefficient of surface tension must be included as a parameter. In the present case, the bubble sizes are dependent on surface characteristics. Basically, bubble detachment size is determined by the balance of buoyancy and adhesion forces, akin to detachment bubble sizes in nucleate boiling. In this connection earlier statements (see §2) on interbubble distance are relevant here. Our experience with different electrode materials have shown the electrolysis bubble sizes to be about 150 μm and in the laminar region bubble coalescence and fragmentation are not significant processes. Hence, the surface tension effects are not expected to be important in the development of the present plumes up to the transition point. Another parameter not included explicitly is the gas flow rate Q_g, since from application of the drift flux theory (see Arakeri & Nair 1990) it can be shown that Q_g is proportional to the void fraction, $\epsilon \sim (\rho_l - \rho_p)/(\rho_l - \rho_g)$. Hence, in the present low-void-fraction plumes Q_g and $(\rho_l - \rho_p)$ are not independent and only one of them need be chosen. The four non-dimensional groups which can be formed from the variables mentioned are:

$$\frac{X}{D_0}, \quad \frac{gD_0^3(\rho_l - \rho_g)^2}{\mu^2}, \quad \frac{\rho_l - \rho_p}{\rho_l - \rho_g}, \quad \frac{U_s^2}{gD_0}.$$

If the slip velocity U_s is taken to be of the order of the terminal velocity U_∞, then it turns out that $U_s^2 \ll gD_0$ and the ratio U_s^2/gD_0, which is a Froude number, is unlikely

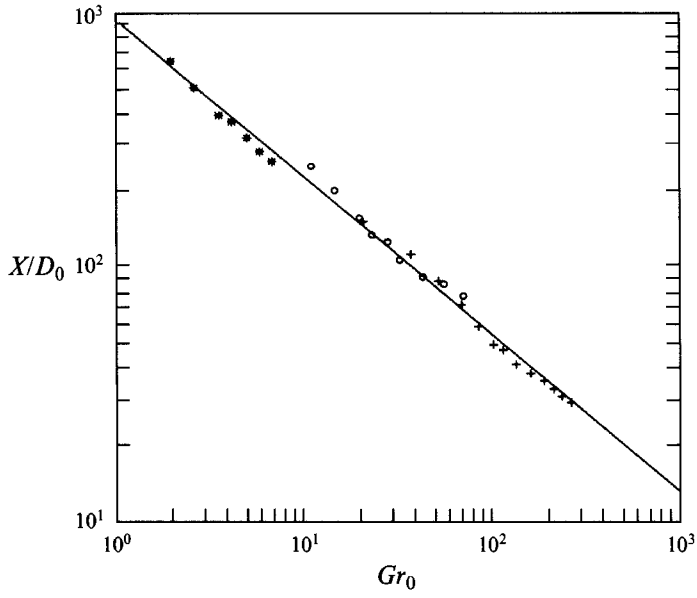

FIGURE 9. Correlation of non-dimensional transition height with source Grashof number: symbols as figure 5.

to be a significant parameter. The ratio $(\rho_l-\rho_p)/(\rho_l-\rho_g)$ is the local void fraction ϵ and is the driving density difference term. Hence the product of the second and the third non-dimensional groups can be interpreted as a local Grashof number, Gr:

$$Gr = \frac{gD_0^3(\rho_l-\rho_g)^2}{\mu^2}\frac{\rho_l-\rho_p}{\rho_l-\rho_g} \approx \frac{gD_0^3}{\nu_l^2}\frac{\Delta\rho}{\rho} = \frac{gD_0^3}{\nu_l^2}\epsilon.$$

In the above, ρ_g is ignored in comparison to ρ_l in replacing $\mu^2/(\rho_l-\rho_g)^2$ by ν_l^2 where ν_l is the liquid kinematic viscosity. Finally, we have looked for a correlation in the form

$$X/D_0 = f(Gr_0),$$

where

$$Gr_0 = \frac{gD_0^3}{\nu_l^2}\epsilon_0 \quad \text{with} \quad \epsilon_0 = Q_g/U_\infty D_0.$$

The Grashof number is now a source Grashof number. As seen from figure 9, there is very good correlation of normalized transition height data with Gr_0 which varies over two orders of magnitude. A straight-line fit to the data in figure 9 gives

$$X/D_0 = 920Gr_0^{-0.61}.$$

It turns out that the source Grashof number based on transition height, Gr_X is not a constant in the present experiments; it varies from 8×10^6 to 5×10^8 for the data in figure 9. Here, Gr_X is $(gX^3/\nu_l^2)\epsilon_0$ and the relationship between Gr_X and Gr_0 follows from the above correlation as $Gr_X = 7.78\times10^8 Gr_0^{-0.83}$. Hence higher Gr_X correspond to lower Gr_0. It is clear that if X/D_0 were proportional to $Gr_0^{-\frac{1}{3}}$, then Gr_X would remain a constant. This appears to be the case for plane thermal plumes in air, where the Grashof number based on transition height and source heat flux has been found to be nearly constant with a magnitude of 8×10^9 (Wakitani & Yosinobu 1988). A cursory examination of the numbers for critical Gr_X suggests that plane bubble plumes are

more unstable than plane thermal plumes in air. However, there are not enough data on transition of thermal plumes in high Prandtl number fluids like water for any meaningful further comparison.

5. Summary

It has been possible to develop an electrolysis technique of generating plane laminar bubble plumes and to study their transitional characteristics. The dominant mode of instability seems to be the sinuous mode where the plume follows a meandering path before breaking up with the formation of discrete vortices in most cases. The relation between transition height X and the wavelength of the most unstable disturbance λ is found to be of the form $X \approx 4\lambda$; in many other cases including thermal plumes the constant of proportionality has been found to be about 10. The measured wave velocity is about 40% of the measured mean plume centreline velocity and this is consistent with single-phase flow results. There is a very good correlation between the normalized transition height data and a source Grashof number. The Grashof number based on transition height is not constant as is suggested by plane thermal plume data in air. It would be useful to carry out further experimental studies along with a numerical simulation based on two-phase flow equations to further understand laminar and transitional flow characteristics of bubble plumes. Some difficulties can be anticipated in the experiments since the present attempts to measure velocity distribution in the liquid region of the plume using LDA were severely hampered owing to the flapping motion of the plume. By conditional averaging it may be possible to overcome these problems.

The authors would like to thank the reviewers for their highly constructive criticism of the original manuscript. They would also like to acknowledge useful discussions on the topic with Drs P. N. Shankar and J. H. Arakeri.

REFERENCES

ALAM, M. 1991 Flow visualization studies on transition and interaction of bubble plumes. MSc (Engng) thesis, Indian Institute of Science, Bangalore.

ARAKERI, V. H. & NAIR, B. G. 1990 Sonic velocity measurements in gas–liquid mixture with low void fractions. *Curr. Sci.* **59**, 363–367.

BAINES, W. D. 1961 The principles of operation of bubbling systems. *Proc. Symp. Air Bubbling, Ottawa. Tech. Mem.* 70, pp. 12–22. National Research Council (Canada).

BILL, R. G. & GEBHART, B. 1975 The transition of plane plumes. *Intl J. Heat Mass Transfer* **18**, 513–528.

BROWN, G. L. & ROSHKO, A. 1974 On density effects and large structure in turbulent mixing layers. *J. Fluid Mech.* **64**, 775–816.

CLIFT, R., GRACE, J. R. & WEBER, M. E. 1978 *Bubbles, Drops and Particles*. Academic.

GORE, R. A., CROWE, C. T. & BEJAN, A. 1990 The geometric similarity of the laminar sections of boundary layer-type flows. *Intl Commun. Heat Transfer* **17**, 465–475.

ISHII, M. 1975 *Thermo-Fluid Dynamic Theory of Two-phase Flow*. Paris: Eyrolles.

JONES, W. T. 1972 Air barriers as oil-spill containment devices. *J. Soc. Petrol. Engng* **12**, 126–142.

KIMURA, S. & BEJAN, A. 1983 Mechanism for transition to turbulence in buoyant plume flow. *Intl J. Heat Mass Transfer* **26**, 1515–1532.

LEITCH, A. M. & BAINES, W. D. 1989 Liquid volume flux in a weak bubble plume. *J. Fluid Mech.* **205**, 77–98.

MCDOUGALL, T. J. 1978 Bubble plumes in stratified environments. *J. Fluid Mech.* **85**, 665–672.

MICHALKE, A. 1965 On spatially growing disturbances in an inviscid shear layer. *J. Fluid Mech.* **23**, 521–544.

MILGRAM, J. H. 1983 Mean flow in round bubble plumes. *J. Fluid Mech.* **133**, 345–376.

SCHORR, A. W. & GEBHART, B. 1970 An experimental investigation of natural convection wakes above a line heat source. *Intl J. Heat Mass Transfer* **13**, 557–571.

TAYLOR, G. I. 1955 The action of a surface current used as a breakwater. *Proc. Roy. Soc.* A **231**, 466–78.

WAKITANI, S. & YOSINOBU, H. 1988 Transition to turbulence in a plane plume above a horizontal line source: measurement of flow properties and flow visualization. *Fluid Dyn. Res.* **2**, 243–259.

WIJNGAARDEN, L. VAN 1972 One-Dimensional Flow of Liquids Containing Small Gas Bubbles. *Ann. Rev. Fluid Mech.* **4**, 369–396.